Quantitative texture analysis in the Texture plugin of SmartLab Studio II

Keigo Nagao* and Akito Sasaki**

1. Introduction

The presence of crystallographic texture (preferred orientation) in polycrystalline materials has a significant effect on the anisotropy of the properties of these materials. That means that quantitative description of the orientation distribution of crystallites, or the orientation distribution function (ODF), is an important task for materials characterization and prediction of their properties. Direct measurement of the ODF is not possible; instead, pole figures (PF) can be measured to determination the ODF. Reconstruction of the ODF from measured PFs is a main goal of quantitative texture analysis. Thus, two problems should be solved to obtain an ODF: measurement and processing of experimental PFs and ODF reconstruction from PFs.

In the X-ray diffraction technique, there are two basic modes for PFs measurement: the conventional mode with a 0D detector and a more advanced mode using a 2D detector[1]. While measurement of PFs with 2D detectors is more advanced, it requires additional tools for conversion of the detector's data into PFs.

When the PFs are prepared, it is possible to start the ODF reconstruction process. Currently, three methods are used for ODF reconstruction: the series expansion method[3], the component method[4, 5], and direct methods like WIMV[6] or ADC[7]. Each method has advantages and disadvantages. The series expansion method is more general, but it requires a large number of measured PFs and has some problems with numerical calculations. The components method represents the ODF as a set of model functions (components) that have clear physical meaning. This method is most convenient for interpretation and representation of the results, but can require a lot of time for selection of components and fitting their parameters. Direct methods use a numerical calculation of the ODF on a discrete grid in rotation space. They are the most simple and convenient to use but do not provide an interpretation of the ODF.

In the next sections we will describe the Texture plugin of SmartLab Studio II, which is intended for data processing and quantitative texture analysis. This plugin implements two of the above-mentioned methods of ODF reconstruction: WIMV and the components methods. Both can be used for all types of crystal systems and two types of sample symmetry—triclinic and orthorhombic. Also, the plugin can use three of the most popular definitions of Eulerian angles in the texture community: Bunge notation (φ_1,Φ,φ_2), Roe notation (Ψ,Θ,Φ) and Matthiers notation (α, β, γ). Roe and Matthiers notation are physically equivalent, with the only difference being the letters used in the notation.

* Application Laboratories, Rigaku Corporation.
** XRD Application & Software Development, Rigaku Corporation.

2. Pole figures processing

The Texture plugin implements advanced algorithms for processing data from 2D detectors. It can process multiple reflections at a time. It is not necessary to define separate areas on the image for diffraction peak background calculation; the background value is estimated from the profile data. The most important advantage is fitting (refinement) of integrated diffraction patterns combined with linear background and Gaussian peak(s). This reduces the defocusing effect (line broadening). Profile fitting is especially useful when processing closely spaced peaks, where it is almost impossible to define the background value. In such a case it is possible to define peaks areas so that they are overlapped and the resulting profile will contain several peaks. Figure 1 shows the result of integration of four close reflection and fitting them as mentioned above. This figure demonstrates that even for "noisy" data this method gives reasonable results.

It is worth noting that it is possible to load datasets for different goniometer settings at the same time. Such datasets cover different parts of the PF, but after processing these parts are combined into a single PF. Figure 2 shows an example of PFs of a Ti sample created from two datasets consisting of 2D maps.

The plugin allows the application of several types of correction, which can be applied individually to each pole figure or to all of them at once. Figure 3 presents the same PFs after a 3° counter-clockwise rotation, orthorhombic symmetrization and normalization. These PFs could be used for ODF calculation.

The texture plugin features a wide variety of graphical abilities for the presentation of PFs. They can be displayed in spherical or cylindrical (projection of hemisphere onto a plane) coordinates. In the latter case, it is possible to use either equal-angle (stereographic) or equal-area (Lambert) projections. For all types of view, values of the PF can be displayed using a color palette or contours.

3. ODF reconstruction

After ODF reconstruction with any method, it is very important to estimate the quality of the reconstruction.

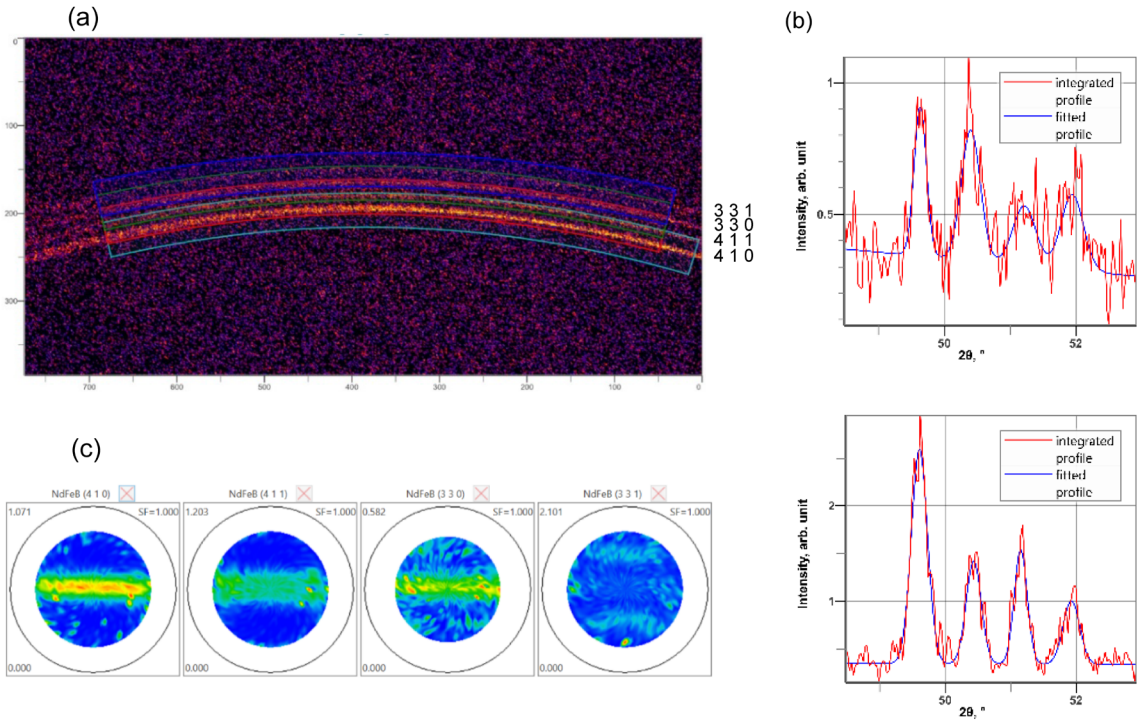

Fig. 1. (a) 2D image of $Nd_2Fe_{14}B$ sample, (b) profile fitting results, (c) measured PFs of (410), (411), (330), and (331).

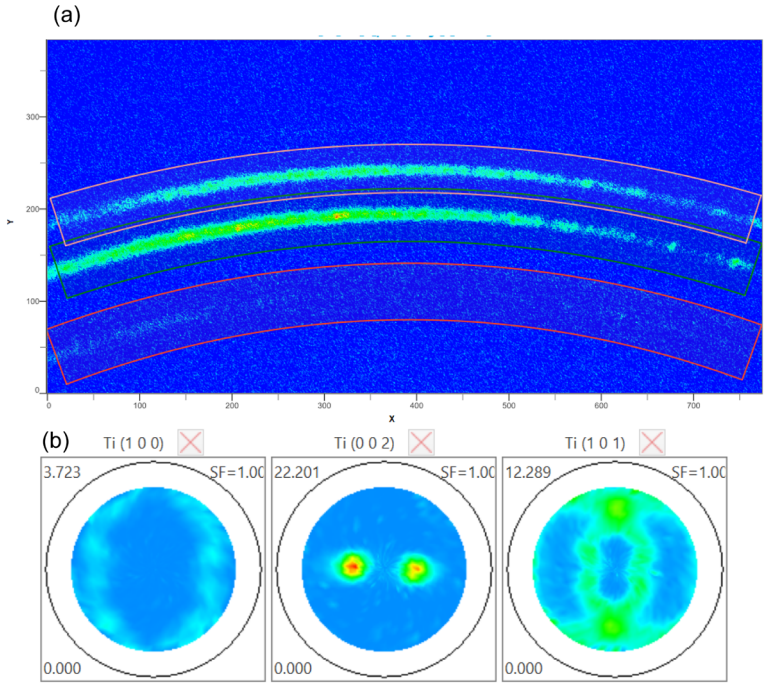

Fig. 2. 2D image of Ti plate (a) and PF data (b).

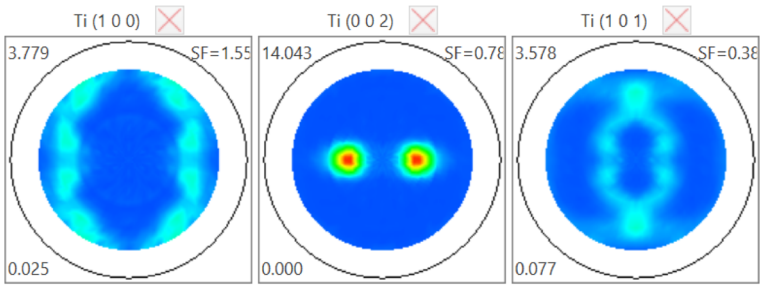

Fig. 3. PF data from Fig. 2 after rotation by 3° anticlockwise, orthorhombic symmetrization, and normalization.

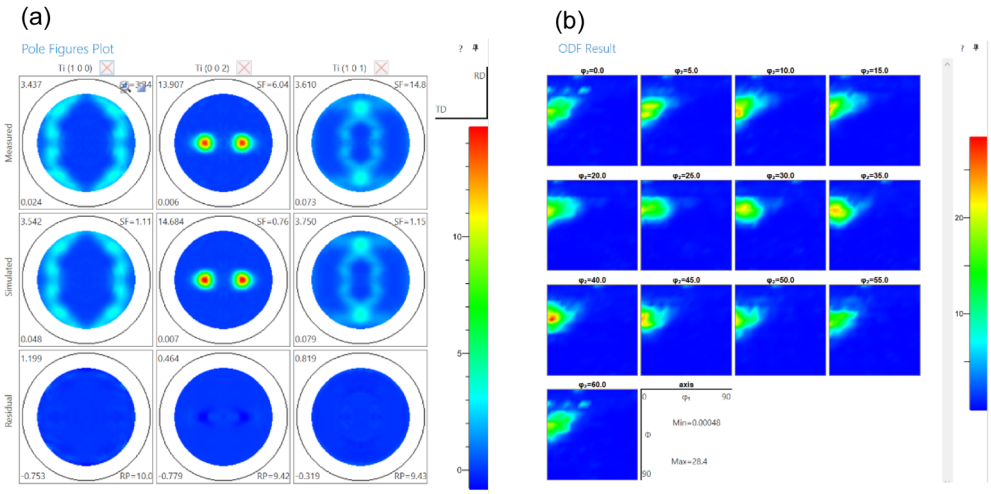

Fig. 4. (a) Measured PF data of Ti plate (top row), recalculated PF data from ODF (second row), and residual PF data (third row). (b) ODF images of Ti plate obtained using the WIMV method ($\varphi 2$ cross-section).

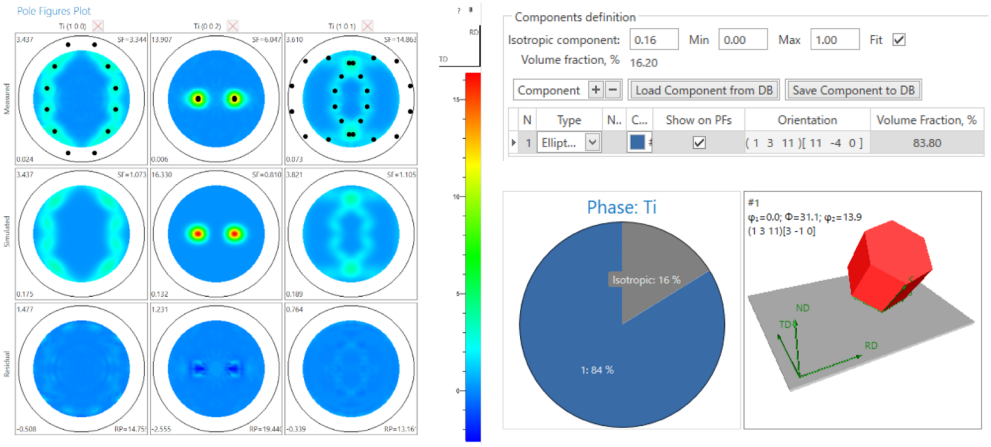

Fig. 5. ODF calculation result and volume fraction calculation of Ti plate sample using the component method.

Usually this estimate is made by comparing measured PFs and PFs that are simulated from the ODF. As a quantitative criterion of quality, the RP factor is used. It is an average of the relative errors between measured and simulated PFs.

3.1. WIMV method

The WIMV method is a direct (purely numerical) method of ODF reconstruction. It calculates values of the function on a discrete grid in 3-dimensional rotation space. From the user's point of view, this is the simplest method because the calculation needs only few parameters. Figure 4 shows the result of a WIMV calculation for the above-mentioned Ti sample. The value of the RP factor in this case is about 9.8%, indicating a good quality reconstruction.

3.2. Components method

The component method is more complicated to use, but gives more representative results. The Texture plugin implements three types of components: spherical (peak), axial (fiber) and elliptical. This method requires the definition of components and an initial approximation for the parameters of each component. If there is no *a priori* information about texture components, this procedure can be quite difficult and time consuming. To overcome this problem, the plugin offer several features. First is components markers, which shows positions of the components' maxima on the pole figures. In Fig. 5 these markers are visible as black points on the experimental PFs. Simply changing the orientation of a component with the mouse allows markers to be aligned with maxima on PFs to estimate initial values for component orientation.

The second important feature is a genetic minimization algorithm. Due to its stochastic nature, this algorithm can find valid component positions even for poorly defined initial approximations. Figure 5 shows an example of an ODF calculation for a Ti sample using one elliptical component and an isotropic component (fraction of randomly oriented crystallites). The initial approximation of the component position was $\varphi_1 = \Phi = \varphi_2 = 0$, which is far from the determined values (2, 32, 43). A solution was found in about 50 seconds

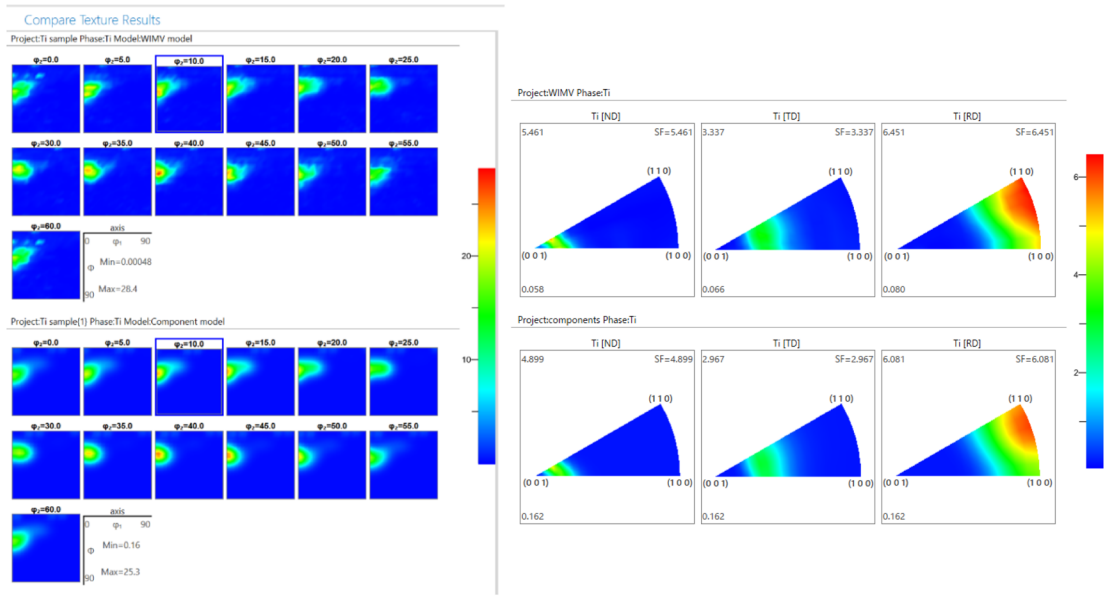

Fig. 6. Comparison of ODF images and IPF data of Ti plate sample using the WIMV method and the component method (top: WIMV, bottom: component).

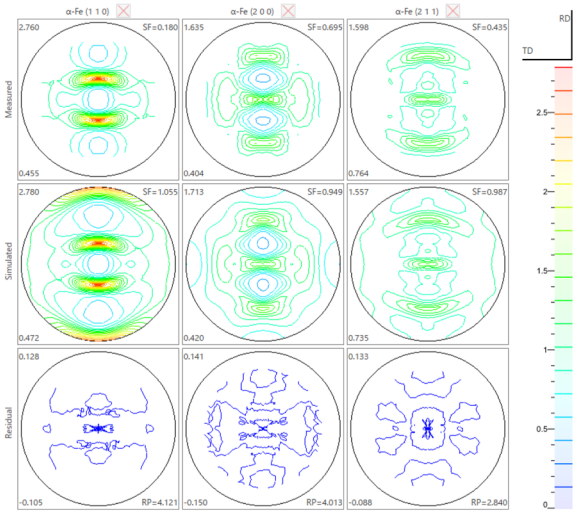

Fig. 7. Measured PFs and recalculated whole PFs obtained from ODF analysis of SPCC using the component method.

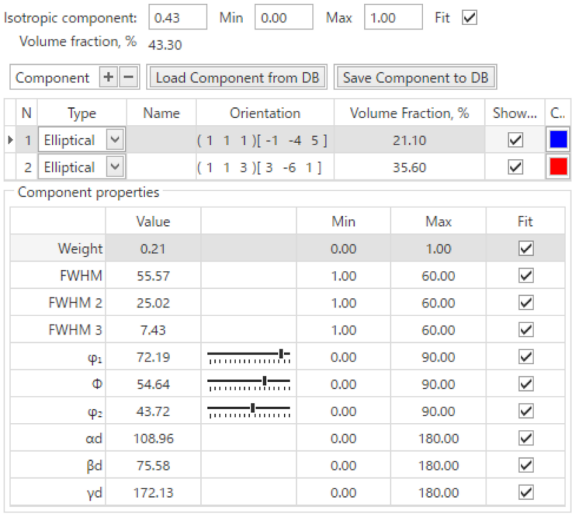

N	Type	Name	Orientation	Volume Fraction, %	Show...	C..
1	Elliptical		(1 1 1)[-1 -4 5]	21.10	☑	
2	Elliptical		(1 1 3)[3 -6 1]	35.60	☑	

	Value		Min	Max	Fit
Weight	0.21		0.00	1.00	☑
FWHM	55.57		1.00	60.00	☑
FWHM 2	25.02		1.00	60.00	☑
FWHM 3	7.43		1.00	60.00	☑
φ1	72.19		0.00	90.00	☑
Φ	54.64		0.00	90.00	☑
φ2	43.72		0.00	90.00	☑
αd	108.96		0.00	180.00	☑
βd	75.58		0.00	180.00	☑
γd	172.13		0.00	180.00	☑

Fig. 8. Refinement parameters used in the component method (ellipsoidal model).

with the help of the genetic minimization algorithm. The obtained solution can be viewed as a pie chart of the volume fraction of components and a graphical representation of the components' orientation. The RP factor in this case is about 17%, which is quite low, but higher than the RP factor from the WIMV calculation. This means that for a more accurate description of the ODF, additional minor components are required.

After the ODF is calculated, it is possible to calculate complete PFs as well as unmeasured PFs. Also, inverse pole figures (IPF) for arbitrary sample directions can be calculated. An additional attractive feature of the Texture plugin is a tool for comparing the ODFs (as well as PFs and IPFs) from different samples. Figure 6 shows ODFs and IPFs, for the above-mentioned Ti sample, calculated with WIMV and Component methods. This tool can be quite convenient, for example, to monitor the change in texture in a sample after various treatments.

4. PF measurement and ODF analysis of steel materials

Figure 7 shows measured PFs and recalculated whole PFs of a 0.5 mm thick cold rolled steel sheet (SPCC). This measurement was made using the Schulz reflection method, with a cobalt radiation source monochromatized by a mirror unit (CBO-α) installed on the incident side. The ODF calculation was analyzed with the genetic minimization algorithm using the component model, with two crystal orientations registered. The poles on the PF showed ring-shaped patterns with intensity distribution, indicating the presence of fiber-like texture. When such patterns are observed, an "elliptical" model

Name	Orientation	Crystal Symmetry
b-2	(0 1 0)[1 0 0]	HEXAGONAL
S	(1 2 3)[6 3 -4]	CUBIC
C-1	(0 0 1)[2 1 0]	HEXAGONAL
C-2	(0 0 1)[1 0 0]	HEXAGONAL
111_pseudo fiber	(1 1 1)[-1 -4 5]	CUBIC
Brass	(1 1 0)[-1 1 2]	CUBIC
Cube	(1 0 0)[0 0 1]	CUBIC
Copper	(1 1 2)[1 1 -1]	CUBIC
b-1	(-1 2 0)[2 1 0]	HEXAGONAL
b-3	(-1 2 0)[0 0 1]	HEXAGONAL
b-4	(0 1 0)[0 0 1]	HEXAGONAL
Taylor	(4 4 11)[11 11 -8]	CUBIC
Goss	(1 1 0)[0 0 1]	CUBIC

Fig. 9. Texture component database.

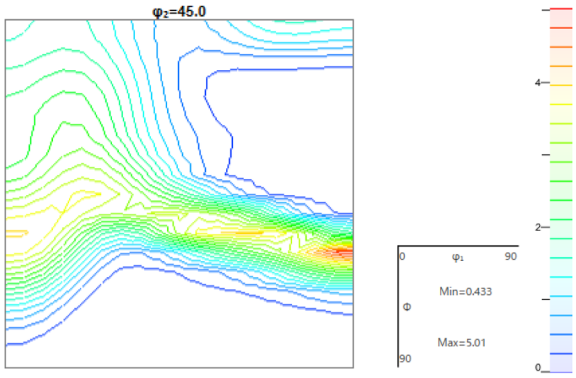

Fig. 10. Crystal orientation distribution map of SPCC ($\varphi 2$: 45° cross-section).

should be chosen as explained in 3.2. In an ellipsoidal model, the polar anisotropy corresponding to the three directions of the Euler angles should be defined by three FWHMs and their orientations (αd, βd, γd) (Fig. 8). The post-refinement RP factor in this setting showed very strong consistency, between 2.8 and 4.1%.

After being refined, the crystal orientation (*hkl*)[*uvw*] is sometimes calculated as a large number, which in many cases is not a generally known crystal orientation. When the ODF calculation is conducted with known crystal orientations, the "fitting" check box of φ_1, Φ, and φ_2 should be unchecked. The Texture plugin has a built-in component database, and well-known crystal orientations for cubic and hexagonal system will be pre-registered upon installation. If you want to reuse refined crystal orientations in the future, you can register them in the component database (Fig. 9).

Figure 10 shows an ODF figure at φ_2: 45°. In general, γ-fiber of steel materials has (111) orientation, and a belt-like pole is observed at Φ: 54.7° and in the direction of φ_1 in the cross-section of φ_2. The γ-fiber-like pole was observed with this sample, too.

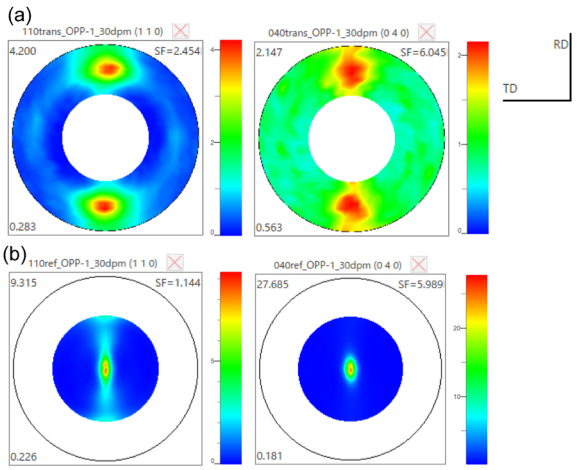

Fig. 11. Transmission PFs (a) and reflection PFs (b) of biaxially stretched PP film.

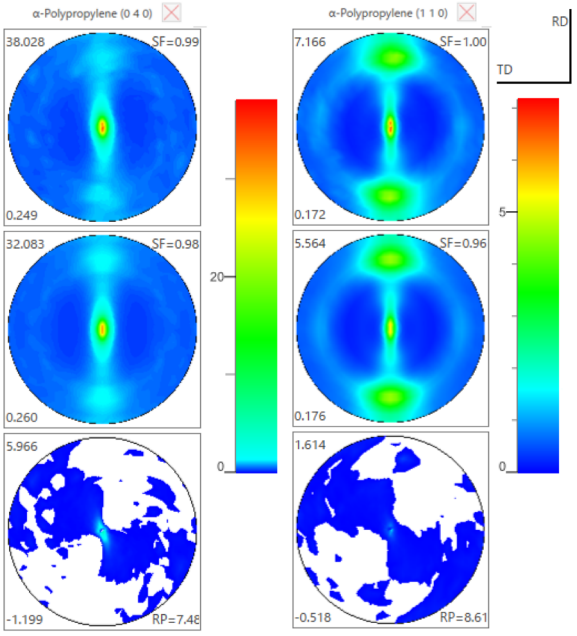

Fig. 12. Connected measured PFs (top), recalculated complete PFs by ODF analysis (using the WIMV method) (middle), and residual PFs (bottom) of biaxially stretched PP film.

5. Measurement of transmission and reflection poles and calculation of orientation function for polymer films

Figure 11 shows transmission and reflection PFs obtained from (110) and (040) of a biaxially stretched polypropylene film (hereinafter referred to as "PP" film). In measuring reflection pole figures, angle α is changed around the χ-axis of the instrument. In measuring transmission pole figures, on the other hand, angle α is controlled by changing the incidence angle ω, with the sample rotated by 90° in the ω direction. 0D-mode measurement was conducted in a parallel-beam optical system using a copper radiation source, with a parallel slit analyzer (PSA) installed on the receiving side. When measuring polymer materials, diffraction peaks are

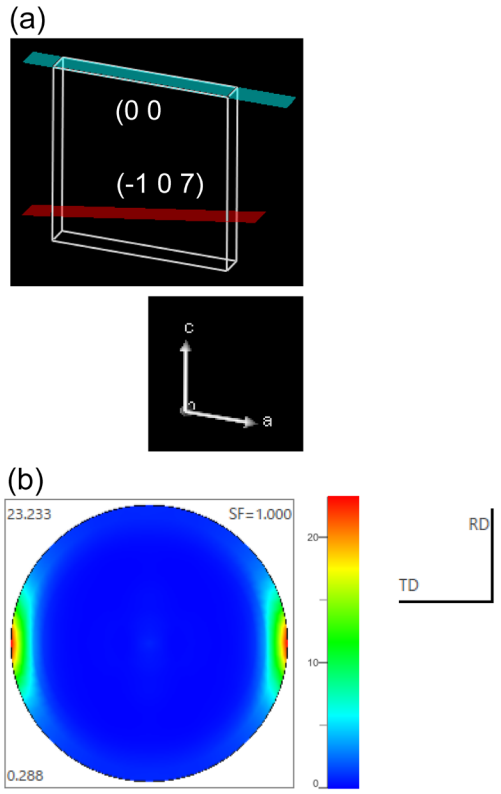

Fig. 13. Crystal structure of PP (a) and recalculated whole PFs of biaxially oriented PP film ($\bar{1}07$) (b).

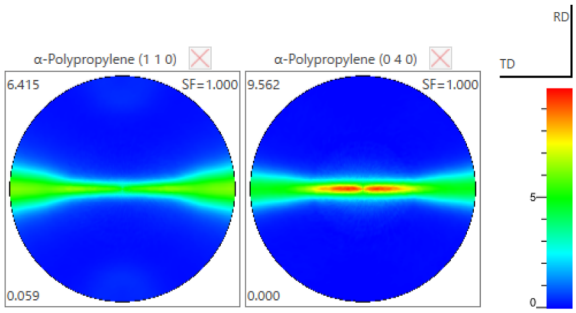

Fig. 14. (110), (040) complete PFs of uniaxially stretched PP film.

densely observed on the low angle side in many cases. The use of a PSA offers the advantage that the width of the diffraction peaks will not change even when χ and ω change. When measuring reflection pole figures, the use of a PSA prevents adjacent diffraction peaks from overlapping with each other when the sample is tilted by the rotation of the χ-axis. The PFs will be connected after completion of background correction, absorption correction, and defocus correction (the latter only for reflection PFs)[2] in each of the transmission PFs and the reflection PFs.

Figure 12 shows the connected whole PFs and the whole PFs recalculated by ODF analysis using the WIMV method. The RP factors were at excellent levels of 10% or below. In polymer orientation analysis, the crystal orientation focusing specifically on the *c*-axis and the degree of the orientation are evaluated. Because the crystal structure of PP is monoclinic, the normal vector of its (001) lattice plane is not parallel with the *c*-axis. For this reason, the orientation and distribution of the *c*-axis cannot be evaluated based on the recalculated whole PF of PP(001). On the other hand, because the normal vector of the ($\bar{1}07$) lattice plane is almost parallel with the *c*-axis, the orientation and distribution levels of the c-axis can be evaluated based on the recalculated PF of ($\bar{1}07$) (Fig. 13).

Table 1. Orientation function of uniaxially and biaxially stretched PP films.

(a) Uniaxially stretched PP.			
	ND	**RD**	**TD**
{0 4 0}	0.406	0.079	0.516
{1 1 0}	0.555	0.032	0.414
a-axis	0.382	0.105	0.513
b-axis	0.555	0.032	0.414
c-axis	0.054	0.885	0.061
(b) Biaxially stretched PP.			
	ND	**RD**	**TD**
{0 4 0}	0.596	0.249	0.155
{1 1 0}	0.312	0.476	0.212
a-axis	0.280	0.493	0.227
b-axis	0.596	0.249	0.155
c-axis	0.120	0.252	0.628

Figure 14 shows the whole PF of a uniaxially stretched PP film. Table 1 shows the orientation function of uniaxially and biaxially stretched PP films. The orientation function can be calculated from whole PFs. This quantitatively expresses the distribution of how strongly the lattice plane normals and the *a*, *b*, *c*-axes are oriented toward the ND, TD and MD (RD)[8, 9]. In the case of the uniaxially stretched PP, the majority of *c*-axes are oriented toward the MD (RD). In the case of the biaxially stretched PP, on the other hand, the majority of *c*-axes are oriented toward the TD. As described above, the use of the orientation function enables the numerical evaluation of crystal orientation and the degree of the distribution in relation to the sample's physical properties and performance.

While an example of PP was presented in this article, this approach can be applied to other types of materials. Analysis of orientation functions can be made for any material, excluding those with a cubic system, by registering their crystal system and lattice constants in the "Material Manager" of the SmartLab Studio II software suite.

6. Summary

In this article, we have presented the Texture plugin (for texture and orientation analysis) of the SmartLab Studio II software suite. This plugin is a full-featured module for analyzing the texture of materials. Because of its ability to analyze both pole figure data measured with 0D detectors and data obtained from 2D

detectors, this Texture plugin is capable of analyzing pole figure data measured using diffractometers in a variety of system configurations. This plugin is designed to significantly facilitate the creation of pole figures from 2D data. In addition, this plugin has two ODF reconstruction methods, enabling highly reliable analysis by selecting the one better-suited for the application. It is expected that this plugin will become a convenient and effective analytical tool in materials development involving orientation control.

References

(1) K. Inaba and S. Kobayashi: *Rigaku Journal (English version)*, **34** (2018), No. 2, 10−16.
(2) K. Nagao and E. Kagami: *Rigaku Journal (English version)*, **27** (2011), No. 2, 6−14.
(3) H. J. Bunge and F. Haessner: *J. Appl. Phys*., **39** (1968), 5503−5514.
(4) G. Wasserman and J. Grewen: *Texturen metallischer Werkstoffe*, Springer, Berlin, (1962).
(5) S. Matthies: *Phys. Status Solidi B,* **101** (1980), K111−K115.
(6) S. Matthies and G. Vinel: *Phys. Status Solidi B,* **112** (1982), K115−K120.
(7) K. Pawlik: *Phys. Status Solidi B*, **134** (1986), 477−483.
(8) P. H. Hermans and P. Platzek: *Kolloid Z.,* **88** (1939), 68.
(9) R. S. Stein: *J. Polymer Sci.,* **31**(1958), 327.